Inorganic Chemistry

Article

pubs.acs.org/IC

Structure–Property Relationships in Solid Solutions of Noncentrosymmetric Aurivillius Phases, $Bi_{4-x}La_xTi_3O_{12}$ (x = 0–0.75)

Seung-Jin Oh,[†] Yiseul Shin,[†] T. Thao Tran,[‡] Dong Woo Lee,[†] Anne Yoon,[§] P. Shiv Halasyamani,[‡] and Kang Min Ok*[,†]

[†]Department of Chemistry, Chung-Ang University, 221 Heukseok-dong, Dongjak-gu, Seoul 156-756, Republic of Korea

[‡]Department of Chemistry, University of Houston, 136 Fleming Building, Houston, Texas 77204-5003, United States

[§]Department of Chemistry, University of Connecticut, 55 North Eagleville Road, Storrs, Connecticut 06269-3188, United States

Supporting Information

ABSTRACT: Solid solutions of the noncentrosymmetric (NCS) Aurivillius phases, $Bi_{4-x}La_xTi_3O_{12}$ (x = 0, 0.25, 0.50, 0.75), have been synthesized through standard solid-state reactions and structurally characterized by powder X-ray and neutron diffractions. These materials crystallize in the orthorhombic space group $B2cb$ (No. 41) and exhibit layered perovskite structures with both $(Bi_2O_2)^{2+}$ fluorite-like units and $[A_{n-1}B_nO_{3n+1}]^{2-}$ (n = 3) blocks. As the amount of La^{3+} cations increases, the polarization arising from the Bi^{3+} positions, especially the A sites of the perovskite units, continuously decreases in the reported materials. Powder second-harmonic generation (SHG) measurements on $Bi_{4-x}La_xTi_3O_{12}$ using 1064 nm radiation revealed frequency-doubling efficiencies ranging from 200 to 50 times that of α-SiO_2. Converse piezoelectric measurements resulted in d_{33} values of 19 and 13 pm V^{-1} for $Bi_4Ti_3O_{12}$ and $Bi_{3.5}La_{0.5}Ti_3O_{12}$, respectively. The magnitudes of the SHG efficiency and piezoelectric response are strongly dependent on the asymmetric coordination environment attributable to the lone pairs on Bi^{3+}. Structure–property relationships along with the influence of the doped foreign cation on the associated NCS properties are discussed.

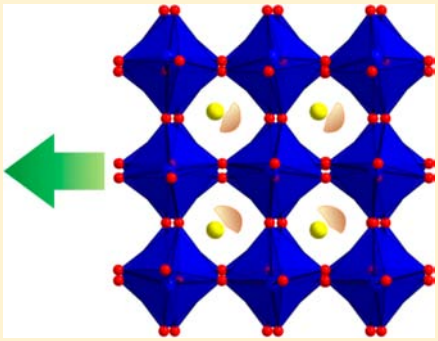

INTRODUCTION

Designing superior performing advanced materials is an ongoing challenge for synthetic chemists. The very essential parts to develop novel functional materials normally include the syntheses, structural determination, and property measurements. Furthermore, the elucidation and understanding of structure–property relationships are considered to be the most fundamental and effective strategies for developing superlative materials continuously. Nowhere is this truer than with noncentrosymmetric (NCS) materials, i.e., compounds lacking an inversion center, since the NCS materials can exhibit a number of technologically important physical properties such as second-harmonic generation (SHG), piezoelectricity, pyroelectricity, and ferroelectricity.[1−6] Thus far, the relationships between NCS structures and the above-mentioned properties are relatively well established.[5,7,8] Specifically, for SHG and piezoelectricity, polarity is not required; however, with pyroelectricity and ferroelectricity, the compounds in question should be polar. One successful approach to increase the macroscopic NCS in materials with extended structures is to introduce cations with an asymmetric coordination environment and larger polarizability. With metal oxides, NCS crystal structures are often observed in compounds containing two families of cations: octahedrally coordinated d^0 transition metals and lone pair cations attributed to second-order Jahn–Teller (SOJT) effects.[9−15] SOJT effects are concerned with structural changes arising from a nondegenerate ground state that interacts with a low-lying excited state. Now the question remains, how can one control the local moments and maximize the macroscopic NCS through aligning the local asymmetric units in a parallel manner? Clearly, it is vital to understand factors determining the macroscopic space group centricity in any new material.[16−19] A few reported key factors that influence the overall centricity include the size of metal cations, hydrogen bonds, and framework flexibility.[20−25]

One interesting family of materials where structure–property relationships can be exploited is in the Aurivillius phases, a class of layered perovskites consisting of fluorite-like $(Bi_2O_2)^{2+}$ units and $[A_{n-1}B_nO_{3n+1}]^{2-}$ blocks. Although the solid solution behavior and a number of interesting physical properties such as ferroelectricity and nonvolatile memory applications of these materials are known,[26−32] a detailed study on the structural origin of the NCS properties was not carried out. In this paper, we report solid-state syntheses, structural characterization, SHG behavior, and piezoelectricity of the $Bi_{4-x}La_xTi_3O_{12}$ (x = 0, 0.25, 0.50, 0.75) solid solutions. In addition, we discuss structure–property relationships and examine the influence of the doped foreign cation on the associated NCS properties of the materials.

Received: July 24, 2012
Published: September 17, 2012

   dx.doi.org/10.1021/ic301615f | Inorg. Chem. 2012, 51, 10402–10407

Table 1. Summary of Crystallographic Data and Refinement Results for $Bi_{4-x}La_xTi_3O_{12}$

	X-ray diffractions				neutron diffraction
formula	$Bi_4Ti_3O_{12}$	$Bi_{3.75}La_{0.25}Ti_3O_{12}$	$Bi_{3.5}La_{0.5}Ti_3O_{12}$	$Bi_{3.25}La_{0.75}Ti_3O_{12}$	$Bi_{3.5}La_{0.5}Ti_3O_{12}$
space group	*B2cb* (No. 41)	*B2cb* (No. 41)	*B2cb* (No. 41)	*B2cb* (No. 41)	*B2cb* (No. 41)
a (Å)	5.44638(10)	5.43976(9)	5.43291(9)	5.42389(8)	5.43461(13)
b (Å)	5.40961(10)	5.41021(9)	5.41426(9)	5.41490(9)	5.41240(13)
c (Å)	32.8243(5)	32.8304(4)	32.8501(3)	32.8804(4)	32.8816(8)
V (Å^3)	967.10(3)	966.27(3)	966.29(3)	965.69(3)	967.19(4)
λ (Å)	1.5406	1.5406	1.5406	1.5406	1.83426
R_p[a]	0.0690	0.0696	0.0716	0.0714	0.0542
R_{wp}[b]	0.0899	0.0920	0.0941	0.0931	0.0698

[a] $R_p = \Sigma|I_o - I_c|/\Sigma I_o$. [b] $R_{wp} = [\Sigma w\,|I_o - I_c|^2/\Sigma w I_o^2]^{1/2}$.

EXPERIMENTAL SECTION

Synthesis. $Bi_{4-x}La_xTi_3O_{12}$ (x = 0, 0.25, 0.50, 0.75) phases were synthesized through standard solid-state reactions. La_2O_3 was dried overnight at 1100 °C before being used. Stoichiometric amounts of Bi_2O_3 (Alfa Aesar, 99%), La_2O_3 (Wako Pure Chemical, 99.99%), and TiO_2 (Kanto Chemical, 99.5%) were thoroughly mixed with an agate mortar and pestle and pressed into pellets. Pellets in alumina crucibles were gradually heated to 750 °C for 24 h, 850 °C for 24 h, and 1000 °C for 24 h with intermediate regrindings. All samples were cooled back, reground, and repelletized during intermediate heatings. Samples were cooled at a rate of 10 °C h^{-1} to room temperature.

Powder X-ray and Neutron Diffractions. Powder X-ray diffraction data were collected on a Bruker D8-Advance diffractometer using Cu Kα radiation at room temperature with 40 kV and 40 mA. The 2θ range was 10−100° with a step size of 0.02° and a step time of 1 s. Neutron diffraction data were obtained at room temperature over the 2θ range of 5−140° with a step size of 0.05° on a high-resolution powder diffractometer (HRPD), where a neutron source with λ = 1.83426 Å supplied by a Ge(331) single-crystal monochromator was used at HANARO Center, KAERI, Korea. Diffraction patterns were analyzed using the Rietveld method with the GSAS program.[33] Structural refinement of the materials was carried out in the space group *B2cb* (No. 41) with a starting model of the reported crystal data of $Bi_4Ti_3O_{12}$.[29,34] No crystallographic ordering between the Bi^{3+} and the La^{3+} cations has been observed. Site occupancies for the Bi/La distribution over the two metal sites were refined using the similar split-atom model reported earlier.[32] However, the total occupancy of Bi^{3+}:La^{3+} was fixed to $\{(4-x)/4\}$:$x/4$ as expected from the synthesis. The resulting formulas are in good agreement with the reported stoichiometry. Results of the crystallographic data and refinement results for $Bi_{4-x}La_xTi_3O_{12}$ solid solutions are summarized in Table 1. Atomic positions and isotropic displacement parameters for solid solutions have been deposited in the Supporting Information.

Second-Order Nonlinear Optical (NLO) Measurements. Powder second-harmonic generation (SHG) measurements on polycrystalline $Bi_{4-x}La_xTi_3O_{12}$ were performed on a modified Kurtz-NLO system[35] using 1064 nm radiation. A DAWA Q-switched Nd:YAG laser, operating at 20 Hz, was used for the measurements. Because SHG efficiency has been shown to depend strongly on particle size, polycrystalline samples were ground and sieved (Newark Wire Cloth Co.) into distinct particle size ranges (20−45, 45−63, 63−75, 75−90, 90−125, >125 μm). To make relevant comparisons with known SHG materials, crystalline α-SiO_2 and $LiNbO_3$ were also ground and sieved into the same particle size ranges. Powders with a particle size of 45−63 μm were used for comparing SHG intensities. All of the powder samples with different particle sizes were placed in separate capillary tubes. No index matching fluid was used in any of the experiments. The SHG light, i.e., 532 nm green light, was collected in reflection and detected by a photomultiplier tube (Hamamatsu). In order to detect only the SHG light, a 532 nm narrow band-pass interference filter was attached to the tube. A digital oscilloscope (Tektronix TDS1032) was used to view the SHG signal. A detailed description of the equipment and methodology used has been published.[6]

Piezoelectric Measurements. Converse piezoelectric measurements were performed using a Radiant Technologies RT66A piezoelectric test system with a TREK (model 609E-6) high-voltage amplifier, Precision Materials Analyzer, Precision High Voltage Interface, and MTI 2000 Fotonic Sensor. Polycrystalline $Bi_4Ti_3O_{12}$ and $Bi_{3.5}La_{0.5}Ti_3O_{12}$ were pressed into 13 mm diameter and ∼1.0 mm thick pellets. Pellets were annealed at 1000 °C for 12 h. A conducting silver paste was applied to both sides of the pellet surfaces for electrodes. Maximum voltages of 800−1500 V were applied to the samples. Twenty measurements were performed, and an average was taken.

RESULTS

Structures. The crystal structure of $Bi_4Ti_3O_{12}$ has been reported;[29,34] thus, only a brief structural description will be given here. $Bi_4Ti_3O_{12}$ exhibits the structure of the Aurivillius phase, i.e., a layered perovskite with an intergrowth structure composed of both $(Bi_2O_2)^{2+}$ rock-salt units and $[A_{n-1}B_nO_{3n+1}]^{2-}$ (n = 3) blocks (see Figure 1). $Bi_4Ti_3O_{12}$ crystallizes in a noncentrosymmetric space group *B2cb* (No. 41) at room temperature attributable to the displacements of Bi^{3+} cations with corresponding tilting and distortion of TiO_6 octahedra. There are two symmetrically unique Ti^{4+} cations that are bonded to six oxygen atoms in distorted octahedral coordination environments with bond lengths ranging from 1.71(2) to 2.27(2) Å. There are also two symmetrically unique Bi^{3+} cations in $Bi_4Ti_3O_{12}$; while the A site of the perovskite block is occupied by the $Bi(1)^{3+}$ cation, the $Bi(2)^{3+}$ cation resides in the $(Bi_2O_2)^{2+}$ rock-salt unit. The Bi−O contact distances range from 2.17(10) to 3.28(3) Å. We chose to substitute up to x = 0.75 of La^{3+} cation for Bi^{3+} to form solid solutions, i.e., $Bi_{4-x}La_xTi_3O_{12}$ (x = 0.25, 0.50, and 0.75). Although no evidence for ordering was observed, the Bi^{3+} in the A site of the perovskite block tends to be preferentially substituted compared to the $(Bi_2O_2)^{2+}$ rock-salt unit. This similar site preference behavior for the La^{3+} cation has been observed before.[36,37] The experimental, calculated, and difference X-ray and neutron diffraction plots for $Bi_{3.5}La_{0.5}Ti_3O_{12}$ are shown in Figure 2. Diffraction plots along with atomic positions and isotropic displacement parameters for all other solid solutions have been deposited to the Supporting Information.

Second-Order Nonlinear Optical (NLO) Measurements. Because $Bi_{4-x}La_xTi_3O_{12}$ solid solutions crystallize in a noncentrosymmetric (NCS) space group, the second-order nonlinear optical (NLO) properties were investigated. Powder SHG measurements on $Bi_4Ti_3O_{12}$, using 1064 nm radiation, indicated the material has SHG efficiency of approximately 200 times that of α-SiO_2. However, as the amount of La^{3+} cation in $Bi_{4-x}La_xTi_3O_{12}$ increases to x = 0.25, 0.50, and 0.75, the SHG efficiencies decrease to 160, 100, and 50 times that of α-SiO_2,

dx.doi.org/10.1021/ic301615f | Inorg. Chem. 2012, 51, 10402−10407

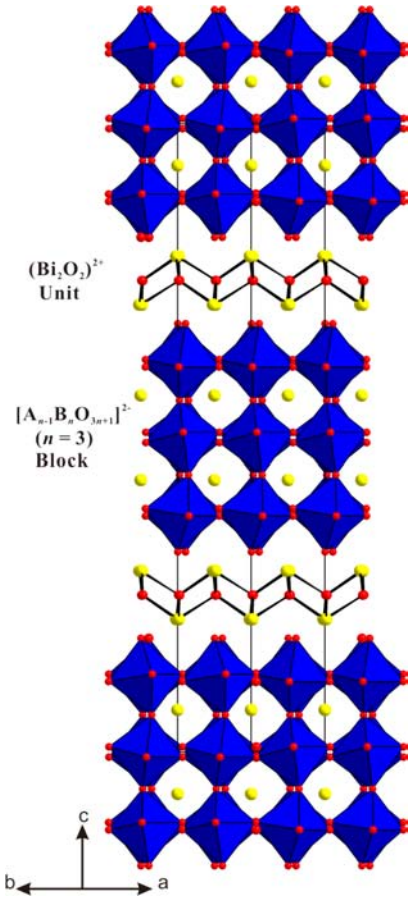

Figure 1. Ball-and-stick and polyhedral representation of $Bi_4Ti_3O_{12}$ viewed along the [110] direction. Aurivillius phase structure composed of $(Bi_2O_2)^{2+}$ rock-salt units and $[A_{n-1}B_nO_{3n+1}]^{2-}$ (n = 3) blocks is observed (blue, Ti; yellow, Bi; red, O).

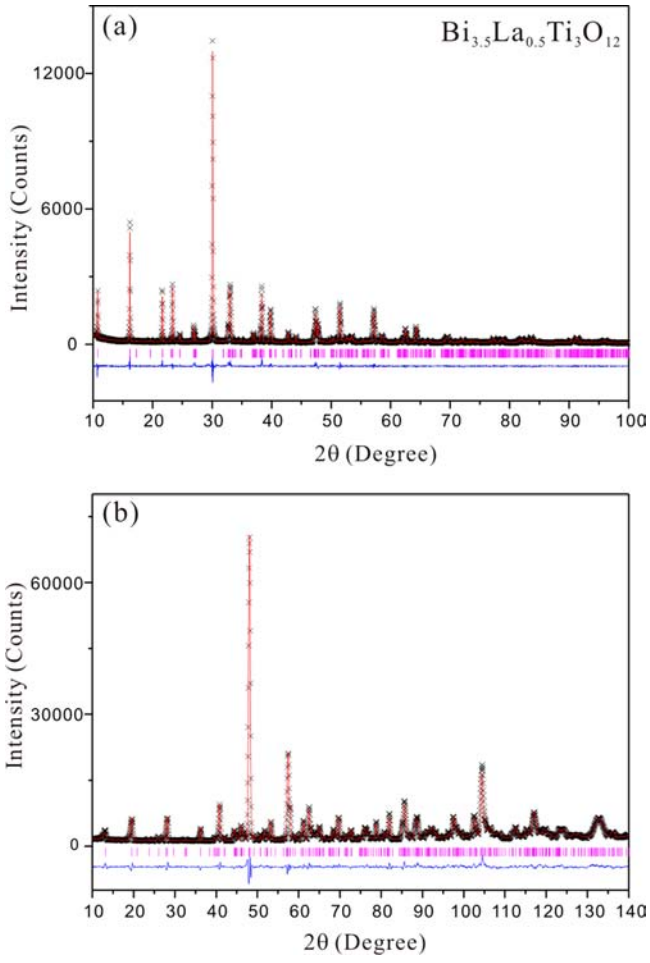

Figure 2. Experimental, calculated, and difference (a) X-ray and (b) neutron diffraction plots for $Bi_{3.5}La_{0.5}Ti_3O_{12}$. Calculated pattern (red solid line) is compared with observed data (×). Locations of reflections are indicated by the magenta vertical bars. Difference between the observed and the calculated profiles is shown at the bottom (blue solid line).

respectively. By sieving the powder samples of $Bi_4Ti_3O_{12}$ and $Bi_{3.5}La_{0.5}Ti_3O_{12}$ into various particle sizes, ranging from 20−150 μm, and measuring the SHG as a function of particle size, we were also able to determine the Type 1 phase-matching capabilities of the materials. We determined that both $Bi_4Ti_3O_{12}$ and $Bi_{3.5}La_{0.5}Ti_3O_{12}$ are not phase matchable. The phase-matching curves for $Bi_4Ti_3O_{12}$ and $Bi_{3.5}La_{0.5}Ti_3O_{12}$ have been deposited to the Supporting Information. On the basis of the powder SHG efficiencies and phase-matching measurements, $Bi_4Ti_3O_{12}$ and $Bi_{3.5}La_{0.5}Ti_3O_{12}$ can be classified as the class C category of SHG materials, as defined by Kurtz and Perry.[35] The measured SHG efficiencies and phase-matching behaviors allowed us to calculate the bulk SHG efficiency, $\langle d_{eff}\rangle_{exp}$, for each material.[38] The $\langle d_{eff}\rangle_{exp}$ values for $Bi_4Ti_3O_{12}$ and $Bi_{3.5}La_{0.5}Ti_3O_{12}$ are approximately 7.8 and 5.5 pm V^{-1}.

Piezoelectric Measurements. Converse piezoelectric measurements were performed on $Bi_4Ti_3O_{12}$ and $Bi_{3.5}La_{0.5}Ti_3O_{12}$. In these measurements, application of a voltage results in macroscopic deformation of the material, which in turn is occurring as a strain parallel to the direction of the polarization. Maximum voltages of 800−1500 V were applied to the samples. For each material, 20 measurements were performed and an average was taken. Plots of the piezoelectric data have been deposited in the Supporting Information. The piezoelectric charge constant, d_{33}, was calculated from

$$\Delta L = SL_0 \sim Ed_{33}L_0$$

where ΔL is the displacement of the sample, L_0 is the sample thickness (m), S is the strain ($\Delta L/L_0$), and E is the electric field strength (V m^{-1}). We estimate d_{33} values of 19 and 13 pm V^{-1} for $Bi_4Ti_3O_{12}$ and $Bi_{3.5}La_{0.5}Ti_3O_{12}$, respectively. Values are similar to that of $LiNbO_3$ (d_{33} = 6−19 pm V^{-1}).[39] The measured acentric data for $Bi_4Ti_3O_{12}$ and $Bi_{3.5}La_{0.5}Ti_3O_{12}$ are given in Table 2.

Discussion. The observed acentric physical properties such as SHG and piezoelectricity can be explained by analyzing how the local asymmetric coordination polyhedra bond, interact, and constructively add. In other words, the origin and

Table 2. SHG and Piezoelectric Data for $Bi_4Ti_3O_{12}$ and $Bi_{3.5}La_{0.5}Ti_3O_{12}$

compound	SHG efficiency (×α-SiO_2)	phase matching	$\langle d_{eff}\rangle_{exp}$ (pm V^{-1})	piezoelectric coefficient d_{33} (pm V^{-1})
$Bi_4Ti_3O_{12}$	200	NPM[a]	7.8	19
$Bi_{3.5}La_{0.5}Ti_3O_{12}$	100	NPM	5.5	13

[a]NPM = Type 1, nonphase matchable.

dx.doi.org/10.1021/ic301615f | Inorg. Chem. 2012, 51, 10402−10407

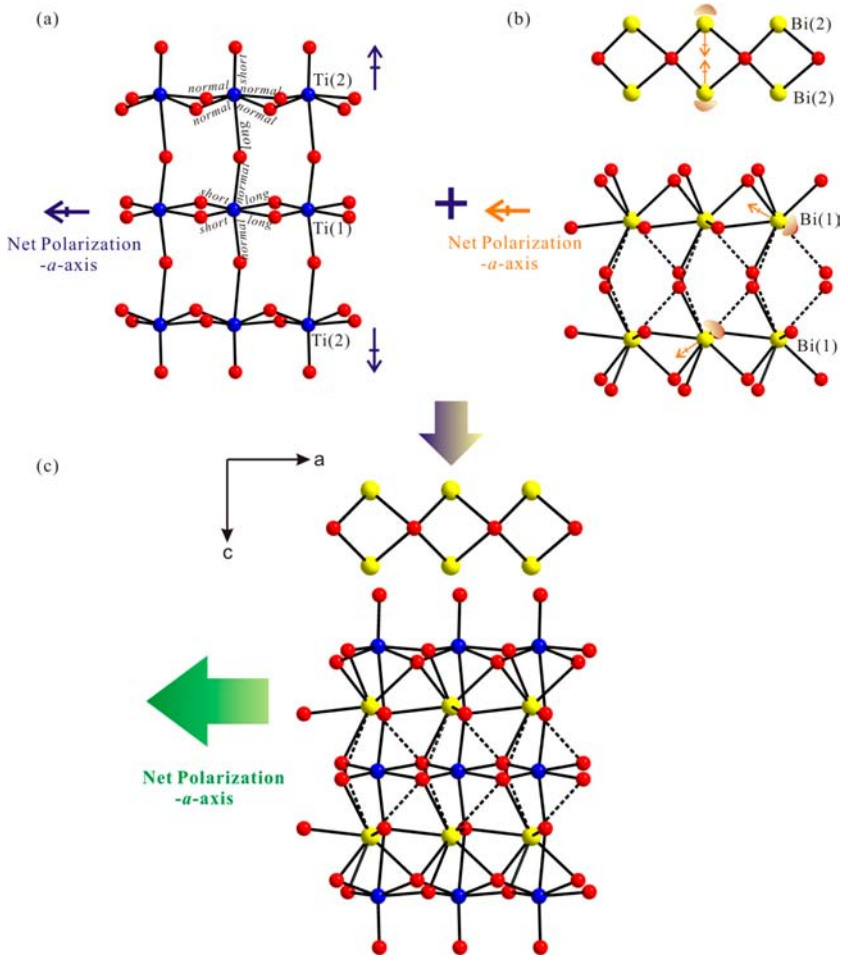

Figure 3. Net polarization arising from the (a) Ti^{4+} cations, (b) Bi^{3+} cations, and (c) overall structure in $Bi_{4-x}La_xTi_3O_{12}$. Note that $Ti(1)O_6$ octahedra have a C_2 distortion along the [−100] direction, whereas $Ti(2)O_6$ octahedra have C_4 distortions along the [001] and [00−1] directions. A moment arising from the Bi^{3+} cations is also observed toward the [−100] direction. Once taking the moments from both Ti^{4+} and Bi^{3+} as a whole, a net polarization is generated toward the [−100] direction.

magnitude of the NCS properties can be understood by determining the macroscopic net direction of the polarizations of the materials. In $Bi_{4-x}La_xTi_3O_{12}$ solid solutions, both kinds of SOJT distortive cations, Ti^{4+} and Bi^{3+} may contribute toward the asymmetric functionality. First, the two octahedrally coordinated Ti^{4+} cations are asymmetrically bonded to six oxygen atoms attributable to SOJT effects as seen in Figure 3a. Edge-type (local C_2 direction) and corner-type (local C_4 direction) distortions are observed for $Ti(1)O_6$ and $Ti(2)O_6$ octahedra, respectively. In fact, with Ti^{4+}, only C_2 (edge) and C_4 (corner) displacements have been observed.[40] For $Ti(1)^{4+}$, two "short", two "long", and two "intermediate" Ti(1)−O bonds are observed. Thus, a moment is generated toward the [−100] direction from the $Ti(1)O_6$ octahedra (see Figure 3a). Meanwhile, one "short" and one "long" Ti−O bonds trans to each other, with four "normal" Ti−O bonds are observed from the $Ti(2)O_6$ octahedra. The moment associated with $Ti(2)O_6$ octahedra, however, is zero, because the polarization on the $Ti(2)O_6$ octahedra alternates between the [001] and the [00−1] directions (see Figure 3a). Thus, a net polarization generated from the TiO_6 octahedra is toward the [−100] direction. Second, each Bi^{3+} cation also is in an asymmetric coordination environment attributable to the lone pair. As seen in the Figure 3b, $Bi(1)^{3+}$ and $Bi(2)^{3+}$ cations are observed from the perovskite blocks and $(Bi_2O_2)^{2+}$ rock-salt units, respectively. The lone pairs on the asymmetric $Bi(1)^{3+}$ cations approximately point toward the [101] and [10−1] directions. Since the local moment for the $Bi(1)O_8$ groups points in the opposite direction of the lone pair, a polarization in the [−100] direction attributable to the alignment of lone pairs on $Bi(1)^{3+}$ cations is observed (see Figure 3b). Meanwhile, the lone pairs on the $Bi(2)^{3+}$ cations point approximately toward the [001] and [00−1] directions; thus, the moment associated with $Bi(2)^{3+}$ cations almost cancels. Therefore, a net moment arising from the Bi^{3+} cations is also observed toward the [−100] direction. Once taking the moments from both Ti^{4+} and Bi^{3+} as a whole, a net moment is observed along the [−100] direction (Figure 3c). In fact, the only symmetry-allowed polarization direction is down the *a* axis based on the space group, *B*2*cb*, which is consistent with our observation. This net moment must be responsible for the observed NCS properties of $Bi_{4-x}La_xTi_3O_{12}$ solid solutions.

The SHG behavior of the $Bi_{4-x}La_xTi_3O_{12}$ solid solutions is shown in Figure 4. As seen in Figure 4, the SHG efficiency deceases as more La^{3+} is doped to the solid solutions. Similarly, the piezoelectric charge constants, d_{33}, decrease from 19 to 13 pm V^{-1} for $Bi_4Ti_3O_{12}$ and $Bi_{3.5}La_{0.5}Ti_3O_{12}$, respectively. The reduction in SHG and piezoelectricity is consistent with the lack of net polarization arising from the polyhedra for the Bi^{3+} cation. As we indicated earlier, Bi^{3+} and La^{3+} are disordered over the two metal sites. In fact, the lone pair cation Bi^{3+} is

dx.doi.org/10.1021/ic301615f | *Inorg. Chem.* 2012, 51, 10402−10407

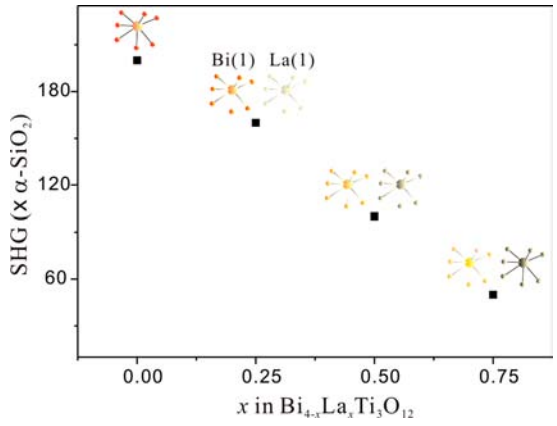

Figure 4. SHG vs La^{3+} doping in $Bi_{4-x}La_xTi_3O_{12}$. Note the SHG efficiency decreases as more La^{3+} is doped to the solid solutions.

favored in the square-antiprismatic rock-salt unit in order to accommodate the asymmetric coordination environment. In other words, more La^{3+} cations that do not contain asymmetric coordination environments occupy the A site of the perovskite block as we increase x in the $Bi_{4-x}La_xTi_3O_{12}$ solid solutions. Refined occupancies reveal that the amount of Bi^{3+} in the A site (Bi(1) site) decrease continuously. The values are 0.934(5), 0.851(5), and 0.712(5) for x = 0.25, 0.50, and 0.75, respectively. Although a small amount of La^{3+} is observed in the fluorite-like unit, most of the Bi(2) sites are occupied by the Bi^{3+} attributable to the preference of the square-antiprismatic coordination environment for the lone pair cations (see the Supporting Information). Also, strain caused by the central environment of La^{3+} in the Bi(2) site may result in a marked preference of Bi^{3+} for the fluorite block.[32] Accordingly, the net polarization will diminish and the NCS properties decrease as La^{3+} is substituted for the polarized cation, Bi^{3+}. As we will discuss more in detail later, however, the local dipole moment calculations indicate that inclusion of a nonpolarizable cation, La^{3+}, does not profoundly influence polarization of TiO_6 octahedra. No significant change of dipole moments on the TiO_6 octahedra is observed, even though the Bi^{3+} cation is continuously replaced by La^{3+} (see below). In fact, it is not surprising to observe the similar dipole moments on the TiO_6 octahedra in a series of different $Bi_{4-x}La_xTi_3O_{12}$ solid solutions, since the cation sizes of Bi^{3+} and La^{3+} are quite similar. The ionic radii of eight-coordinate Bi^{3+} and La^{3+} are known to be 1.17 and 1.16 Å, respectively.[41] Thus, the degree of distortions of TiO_6 octahedra would be almost the same, although foreign cations with similar size are introduced to the A site of the $[A_{n-1}B_nO_{3n+1}]^{2-}$ block.

In order to better understand the asymmetric coordination environment, we calculated the local dipole moments for Ti^{4+} and Bi^{3+} in $Bi_{4-x}La_xTi_3O_{12}$ solid solutions. This approach has been described earlier with respect to metal oxyfluoride octahedra.[42,43] We found that the local dipole moments for $Bi(1)O_8$ and $Bi(2)O_6$ polyhedra range from about 6.14 to 7.80 and 6.59 to 7.94 D (D = Debyes), respectively. Also, the local dipole moments for the $Ti(1)O_6$ and $Ti(2)O_6$ octahedra in the reported materials exhibit values ranging from about 4.20 to 5.45 and 7.29 to 10.44 D, respectively. No substantial change of dipole moment of TiO_6 octahedra has been observed, although the amount of La^{3+} increases. A complete calculation of dipole moments for the constituted polyhedra is listed in Table 3.

Table 3. Calculation of Dipole Moments for BiO_6, BiO_8, and TiO_6 Polyhedra

compound	species	dipole moment (D)
$Bi_4Ti_3O_{12}$	$Ti(1)O_6$	4.20
	$Ti(2)O_6$	7.29
	$Bi(1)O_8$	6.14
	$Bi(2)O_6$	7.94
$Bi_{3.75}La_{0.25}Ti_3O_{12}$	$Ti(1)O_6$	5.37
	$Ti(2)O_6$	9.89
	$Bi(1)O_8$	7.43
	$Bi(2)O_6$	6.59
$Bi_{3.5}La_{0.5}Ti_3O_{12}$	$Ti(1)O_6$	5.45
	$Ti(2)O_6$	9.69
	$Bi(1)O_8$	7.80
	$Bi(2)O_6$	6.81
$Bi_{3.5}La_{0.5}Ti_3O_{12}$ (neutron)	$Ti(1)O_6$	4.75
	$Ti(2)O_6$	10.44
	$Bi(1)O_8$	6.42
	$Bi(2)O_6$	6.69
$Bi_{3.25}La_{0.75}Ti_3O_{12}$	$Ti(1)O_6$	4.96
	$Ti(2)O_6$	10.14
	$Bi(1)O_8$	7.10
	$Bi(2)O_6$	6.59

CONCLUSIONS

We successfully synthesized a series of NCS Aurivillius phases, $Bi_{4-x}La_xTi_3O_{12}$ (x = 0, 0.25, 0.50, 0.75) solid solutions, by standard solid-state reactions. The materials were structurally characterized by powder X-ray and neutron diffractions and analyzed using a Rietveld method. Powder SHG measurements on $Bi_{4-x}La_xTi_3O_{12}$ using 1064 nm radiation indicate the materials are nonphase matchable (Type 1) with SHG efficiencies approximately ranging from 50 to 200 times that of α-SiO_2. Converse piezoelectric measurements revealed d_{33} values of 19 and 13 pm V^{-1} for $Bi_4Ti_3O_{12}$ and $Bi_{3.5}La_{0.5}Ti_3O_{12}$, respectively. We determined that the NCS properties of $Bi_{4-x}La_xTi_3O_{12}$ decrease upon addition of La^{3+} to the solid solutions. Inclusion of a nonpolarizable cation, La^{3+}, to solid solutions is detrimental to the acentric properties. We are in the process of synthesizing other new NCS mixed-metal oxide materials and will be reporting on them shortly.

ASSOCIATED CONTENT

Supporting Information

X-ray diffraction data (calculated, experimental, and difference), atomic coordinates, SHG phase-matching plots, and piezoelectric measurements data for $Bi_{4-x}La_xTi_3O_{12}$ (x = 0, 0.25, 0.50, 0.75). This material is available free of charge via the Internet at http://pubs.acs.org.

AUTHOR INFORMATION

Corresponding Author

*Phone: +82-2-820-5197. Fax: +82-2-825-4736. E-mail: kmok@cau.ac.kr.

Notes

The authors declare no competing financial interest.

ACKNOWLEDGMENTS

This research was supported by the Basic Science Research Program through the National Research Foundation of Korea (NRF) funded by the Ministry of Education, Science &

Technology (grant 2010-0002480). P.S.H. and T.T.T. thank the Welch Foundation (Grant E-1457) and the Texas Center for Superconductivity for support.

REFERENCES

(1) Nye, J. F. *Physical Properties of Crystals*; Oxford University Press: Oxford, U.K., 1957.
(2) Jona, F.; Shirane, G. *Ferroelectric Crystals*; Pergamon Press: Oxford, 1962.
(3) Cady, W. G. *Piezoelectricity; an Introduction to the Theory and Applications of Electromechanical Phenomena in Crystals*; Dover: New York, 1964.
(4) Lang, S. B. *Sourcebook of Pyroelectricity*; Gordon & Breach Science: London, 1974.
(5) Halasyamani, P. S.; Poeppelmeier, K. R. *Chem. Mater.* **1998**, *10*, 2753.
(6) Ok, K. M.; Chi, E. O.; Halasyamani, P. S. *Chem. Soc. Rev.* **2006**, *35*, 710.
(7) Valasek, J. *Phys. Rev.* **1920**, *15*, 537.
(8) Franken, P. A.; Hill, A. E.; Peters, C. W.; Weinreich, G. *Phys. Rev. Lett.* **1961**, *7*, 118.
(9) Opik, U.; Pryce, M. H. L. *Proc. R. Soc. London* **1957**, *A238*, 425.
(10) Bader, R. F. W. *Mol. Phys.* **1960**, *3*, 137.
(11) Bader, R. F. W. *Can. J. Chem.* **1962**, *40*, 1164.
(12) Pearson, R. G. *J. Am. Chem. Soc.* **1969**, *91*, 4947.
(13) Pearson, R. G. *J. Mol. Struct.: THEOCHEM* **1983**, *103*, 25.
(14) Wheeler, R. A.; Whangbo, M.-H.; Hughbanks, T.; Hoffmann, R.; Burdett, J. K.; Albright, T. A. *J. Am. Chem. Soc.* **1986**, *108*, 2222.
(15) Kunz, M.; Brown, I. D. *J. Solid State Chem.* **1995**, *115*, 395.
(16) Kepert, C. J.; Prior, T. J.; Rosseinsky, M. J. *J. Am. Chem. Soc.* **2000**, *122*, 5158.
(17) Maggard, P. A.; Stern, C. L.; Poeppelmeier, K. R. *J. Am. Chem. Soc.* **2001**, *123*, 7742.
(18) Hwu, S.-J.; Ulutagay-Kartin, M.; Clayhold, J. A.; Mackay, R.; Wardojo, T. A.; O'Connor, C. J.; Kraweic, M. *J. Am. Chem. Soc.* **2002**, *124*, 12404.
(19) Welk, M. E.; Norquist, A. J.; Arnold, F. P.; Stern, C. L.; Poeppelmeier, K. R. *Inorg. Chem.* **2002**, *41*, 5119.
(20) Sykora, R. E.; Ok, K. M.; Halasyamani, P. S.; Albrecht-Schmitt, T. E. *J. Am .Chem. Soc.* **2002**, *124*, 1951.
(21) Goodey, J.; Ok, K. M.; Broussard, J.; Hofmann, C.; Escobedo, F. V.; Halasyamani, P. S. *J. Solid State Chem.* **2003**, *175*, 3.
(22) Ok, K. M.; Baek, J.; Halasyamani, P. S.; O'Hare, D. *Inorg. Chem.* **2006**, *45*, 10207.
(23) Choi, M.-H.; Kim, S.-H.; Chang, H. Y.; Halasyamani, P. S.; Ok, K. M. *Inorg. Chem.* **2009**, *48*, 8376.
(24) Lee, D. W.; Bak, D.-b.; Kim, S. B.; Kim, J.; Ok, K. M. *Inorg. Chem.* **2012**, *51*, 7844.
(25) Oh, S.-J.; Lee, D. W.; Ok, K. M. *Inorg. Chem.* **2012**, *51*, 5393.
(26) Aurivillius, B. *Ark. Kemi* **1949**, *1*, 499.
(27) Smolenski, G. A.; Isupov, V. A.; Agranovskaya, A. I. *Sov. Phys. Solid State* **1953**, *3*, 665.
(28) Subbarao, E. C. *J. Phys. Chem. Solids* **1962**, *23*, 665.
(29) Cummins, S. E.; Cross, L. E. *J. Appl. Phys.* **1968**, *39*, 2268.
(30) Paz de Araujo, C. A.; Cuchlaro, J. D.; McMillan, L. D.; Scott, M. C.; Scott, J. F. *Nature* **1995**, *374*, 627.
(31) Park, B. H.; Kang, B. S.; Bu, S. D.; Noh, T. W.; Lee, J.; Jo, W. *Nature* **1999**, *401*, 682.
(32) Hervoches, C. H.; Lightfoot, P. *J. Solid State Chem.* **2000**, *153*, 66.
(33) Larson, A. C.; von Dreele, R. B. *General Structural Analysis System (GSAS)*; Los Alamos National Laboratory: Los Alamos, NM, 1987.
(34) Dorrian, J. F.; Newnham, R. E.; Smith, D. K., Jr. *Ferroelectrics* **1971**, *3*, 17.
(35) Kurtz, S. K.; Perry, T. T. *J. Appl. Phys.* **1968**, *39*, 3798.
(36) Blake, S. M.; Falconer, M. J.; McCreedy, M.; Lightfoot, P. *J. Mater. Chem.* **1997**, *7*, 1609.
(37) Ismunandar; Kennedy, B. J. *J. Mater. Chem.* **1999**, *9*, 541.
(38) Goodey, J.; Broussard, J.; Halasyamani, P. S. *Chem. Mater.* **2002**, *14*, 3174.
(39) In *Numerical Values and Functions from the Natural Sciences and Technology (New Series), Group 3: Crystal and Solid State Physics*; Landolt, H., Ed.; Springer Verlag: Berlin, 1979; Vol. *11*.
(40) Halasyamani, P. S. *Chem. Mater.* **2004**, *16*, 3586.
(41) Shannon, R. D. *Acta Crystallogr.* **1976**, *A32*, 751.
(42) Maggard, P. A.; Nault, T. S.; Stern, C. L.; Poeppelmeier, K. R. *J. Solid State Chem.* **2003**, *175*, 25.
(43) Izumi, H. K.; Kirsch, J. E.; Stern, C. L.; Poeppelmeier, K. R. *Inorg. Chem.* **2005**, *44*, 884.